

Cite this: *J. Mater. Chem. C*, 2023,
11, 5725Realizing near-infrared mechanophosphorescence
from an organic host/guest system†Fei Hao,^a Hailan Wang,^{‡a} Donghai Yu,^a Zhenwei Liu,^a Tiantian Zhang,^b
Mingyao Shen^b and Tao Yu^{*,bc}

Near-infrared mechanoluminescence materials have great potential in higher order encryption and biomechanical visualization *in vivo* because of their unique properties such as biopenetrability and invisibility to the naked-eye. However, organic NIR mechanoluminescence materials remain unexplored. Herein, the design, synthesis and photophysical studies of the first organic host/guest (H/G) NIR mechanoluminescence system with the organometallic complex Pt(II)₂TPPL as the guest and *N*-hexyl carbazole (*N*-hexyl Cz) as the host are reported. Based on the efficient triplet energy transfer and rigid host environment in this H/G system, pure NIR mechanophosphorescence can be detected at 746 nm with high efficiency and the phosphorescence lifetime can be prolonged up to 167 μs when doping 2.0% (w/w) Pt(II)₂TPPL into the *N*-hexyl Cz crystal. Further studies on theoretical calculations have been carried out to gain a deeper understanding of the energy transfer process in this organic H/G system. Additionally, when this material is subjected to a friction, the naked-eye invisible pure NIR mechanophosphorescence could be clearly detected using a NIR camera. This organic H/G NIR mechanophosphorescence material has also demonstrated potential application in higher order encryption and biomechanical visualization due to its naked-eye invisible pure NIR mechanophosphorescence.

Received 9th December 2022,
Accepted 3rd April 2023

DOI: 10.1039/d2tc05253a

rsc.li/materials-c

Introduction

Mechanoluminescence, caused by mechanical stimuli (such as grinding, pressing or stretching), is one of the earliest reported luminescence phenomena.¹ Mechanoluminescent materials have aroused great attention over the past decades because of their potential applications in optoelectronic devices,² anti-counterfeiting,³ real-time sensing for mechanical stress and materials damage,⁴ and light generators driven by naturally vibrating mechanical action,⁵ as well as their environmentally friendly excitation mode.⁶ In recent years, organic mechanoluminescent materials have attracted great attention due to their easy synthesis, low cost, low toxicity and wide luminescence range. Till now, a series of organic/organometallic ML materials have been developed,⁷ such as organic rare earth

metal complexes,⁸ organic transition metal complexes,⁹ carbazole derivatives,¹⁰ phenothiazine derivatives,¹¹ *N*-phenylimide derivatives,¹² tetraphenylethene derivatives,¹³ phosphine (phosphine oxide) derivatives,¹⁴ and borate derivatives.¹⁵ Besides, other materials like aggregation-induced emission (AIE)-based,^{10b,13b,16} thermally activated delayed fluorescence (TADF)-based,^{10b,16a,17} and phosphorescence-based^{11a,15a} materials have also shown good mechanoluminescent properties. However, almost all mechanoluminescence from organic materials was limited to the visible light range. Recently, NIR ML materials, which can penetrate tissues and are invisible to the naked eye, have found potential application in higher order encryption and biomechanical visualization *in vivo*.¹⁸ To the best of our knowledge, only about 12 NIR ML materials have been documented,¹⁸ with all of them being inorganic crystals, while organic mechanoluminescent materials with emission wavelengths in the near-infrared region remain unexplored.

Organic near-infrared light-emitting materials, with $\lambda_{\max} \geq 700$ nm, have attracted great attention due to their widespread applications in night-vision readable displays, information processing and bio-imaging.¹⁹ Till now, organic dyes,^{19i,20} core-enlarged perylene dyes,²¹ fused polycyclic aromatic compounds,²² transition metal complexes^{19h,23} and porphyrinoids^{19h,24} have been developed as NIR materials. Among them, porphyrinoids, which represent porphyrin-related systems, are one of the most investigated classes over the last two decades.²⁵ There have been several types of porphyrinoids demonstrating good NIR luminescence at room temperature, such as Ir(III)-,²⁶ Pt(II)-,^{19h,27} and

^a Shandong Provincial Key Laboratory of Molecular Engineering,
Qilu University of Technology – Shandong Academy of Science, Ji'nan 250353,
China

^b Frontiers Science Center for Flexible Electronics (FSCFE),
Shaanxi Institute of Flexible Electronics (SIFE) & Shaanxi Institute of Biomedical
Materials and Engineering (SIBME), Northwestern Polytechnical University (NPU),
Xi'an 710072, China

^c Key Laboratory of Flexible Electronics of Zhejiang Province,
Ningbo Institute of Northwestern Polytechnical University, 218 Qingyi Road,
Ningbo 315103, China

† Electronic supplementary information (ESI) available. See DOI: <https://doi.org/10.1039/d2tc05253a>

‡ These authors contributed equally to this work.

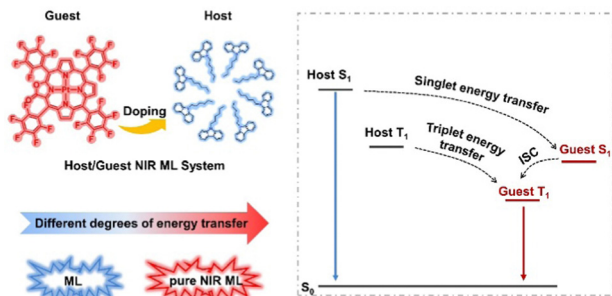


Fig. 1 Schematic illustration of the host/guest NIR ML system.

Pd(II)-porphyrins,^{19h,27a,b,f} Pt(II)-²⁸ and Pd(II)-porphodilactones,²⁸ expanded porphyrins,²⁹ core-modified porphyrins,³⁰ bacteriochlorins,³¹ porphyrin tapes,³² linear porphyrin oligomers³³ and phthalocyanines.³⁴ While many advances in this area have been made, there are ongoing efforts to expand the stimulus type from light to mechanical force and to develop new and efficient NIR mechanoluminescence emitters for the high demands in technological applications. The traditional force-induced fluorescence only uses singlet excitons, leading to 75% of triplet energy produced by electrical excitation being wasted, and the low-level excitons are easily dissipated by non-radiative transitions (Fig. 1). However, mechanophosphorescence could enable high exciton utilization through efficient ISC or RISC conversion and also it possesses a long lifetime which could reduce background interference during stress sensing and material breakage monitoring processes. Therefore, developing novel organic NIR mechanophosphorescence materials is of high demand. Doping guest emitters into rigid matrices to realize various organic ML emitters is a concise, effective and eco-friendly strategy.³⁵ The energy levels could be easily tuned by adjusting energy transfer from the host to the guest. Additionally, a suitable host matrix can prevent triplet energy quenching from ambient humidity and oxygen and provide effective transition pathways for energy transfer between the host and the guest to generate and stabilize triplet excitons. However, a suitable H/G system is difficult to be rationally chosen to realize NIR mechanophosphorescence.

Herein, we report the design, synthesis and photophysical studies of the first organic H/G NIR system (the organometallic complex Pt(II)F₂₀TPPL as the guest and *N*-hexyl Cz as the host; Fig. 1). NIR mechanophosphorescence properties were realized and investigated. Interestingly, different doping ratios of Pt(II)F₂₀TPPL can affect the ML properties of this H/G system. When doping 2.0% (w/w) Pt(II)F₂₀TPPL into the *N*-hexyl Cz crystal, pure NIR mechanophosphorescence can be detected at 746 nm with high efficiency and the phosphorescence lifetime can be prolonged up to 167 μ s, which was realized by efficient triplet energy transfer and the rigid environment of the host. Moreover, theoretical calculations were carried out to gain a deeper understanding of the energy transfer process in this organic H/G system. Additionally, when this material was subjected to a friction, the naked-eye invisible pure NIR mechanophosphorescence could be clearly detected using a NIR camera. Demonstrations of higher order encryption and

biomechanical visualization based on these naked-eye invisible pure NIR mechanophosphorescent materials were also performed.

Results and discussion

First, the organometallic complex Pt(II)F₂₀TPPL was chosen as the guest because it exhibits good emission properties in the NIR region. Besides, the broad excitation range of Pt(II)F₂₀TPPL enables H/G energy transfer. Pt(II)F₂₀TPPL was synthesized by treating H₂F₂₀TPPL with 2 eq. [PtCl₂(PhCN)₂] in anhydrous benzonitrile at 190 °C under a nitrogen atmosphere as reported in the literature.³⁶ The chemical structure of Pt(II)F₂₀TPPL was confirmed by ¹H NMR and MALDI-MS spectroscopy (Fig. S1–S3, ESI†). Since molecular alignment and intermolecular interactions are crucial in mechanoluminescence,³⁷ a series of host matrices with different triplet energy levels and packing modes in the crystalline state were screened, such as benzophenone (BP), thianthrene (TA), triphenylamine (TPA) and *N*-hexyl Cz, as shown in Fig. 2a. Because these matrices are tightly packed in the crystalline state to provide rigid environmental conditions, the twisted molecular structures give them enough space to facilitate the insertion of the guest emitter. These H/G materials can be manufactured by a solvent-less preparation method³⁸ (details are shown in the ESI†), showing the advantages of concise and easy fabrication of the H/G system. To our delight, 1.0% (w/w) Pt(II)F₂₀TPPL dispersed in *N*-alkyl carbazole exhibited intense NIR luminescence under 365 nm UV irradiation. This might be dependent on the ML properties of the *N*-hexyl Cz crystal, which is non-centrosymmetric, possessing the alkyl chain region and loose packing mode, as well as the spectral overlap between the ML emission of the host *N*-hexyl Cz and the absorbance of the guest Pt(II)F₂₀TPPL. It was reported that TPA was chosen as the host matrix in the doping system to generate ML. However, TPA did not work in our doping system. The reason might be that although the TPA crystal does not have ML properties.³⁹

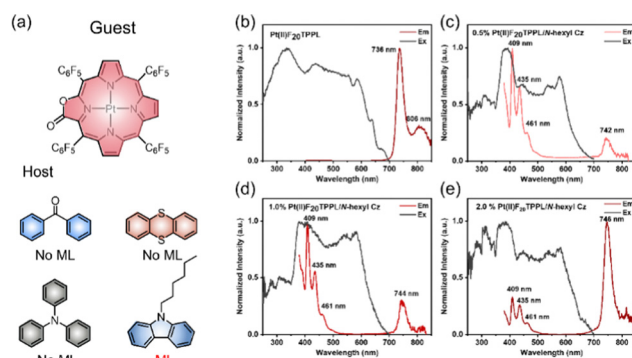


Fig. 2 (a) Chemical structures of the guest emitter Pt(II)F₂₀TPPL and host matrices (BP, TA, TPA, and *N*-hexyl Cz); (b) excitation spectra and steady state PL spectra of Pt(II)F₂₀TPPL, (c) 0.5% Pt(II)F₂₀TPPL/*N*-hexyl Cz, (d) 1.0% Pt(II)F₂₀TPPL/*N*-hexyl Cz and (e) 2.0% Pt(II)F₂₀TPPL/*N*-hexyl Cz ($\lambda_{\text{ex}} = 365$ nm).

Photophysical investigations of pure Pt(II) F_{20} TPPL and the H/G NIR materials with different doping ratios of Pt(II) F_{20} TPPL into *N*-alkyl carbazole were subsequently performed. The corresponding spectra measured under 365 nm excitation at room temperature are shown in Fig. 2b–e. Phosphorescence of pure Pt(II) F_{20} TPPL was detected as a sharp band with the emission maximum at 736 nm, as shown in Fig. 2b. The broad excitation band of Pt(II) F_{20} TPPL indicates its wide applicability in different excitation sources. The photoluminescence processes of the H/G systems with different doping ratios were all detected as two major emission bands at corresponding wavelengths. When the doping ratio was changed from 0.5% to 2.0%, the emission band at *ca.* 409 nm (originating from *N*-hexyl Cz) was significantly reduced and the emission band at *ca.* 746 nm was drastically enhanced. Compared with the solid state emission of Pt(II) F_{20} TPPL, a slight red-shift was observed in the H/G system. This might be attributed to the rigid environment of the host matrices. The crystallinity of *N*-hexyl carbazole, Pt(II) F_{20} TPPL and *N*-hexyl carbazole/Pt(II) F_{20} TPPL doped materials was characterized by X-ray diffraction (Fig. S4, ESI†). Moreover, the time-resolved decay curves of these H/G NIR materials were measured at room temperature and are presented in the ESI† (Fig. S6 and S7). The phosphorescence lifetime extended obviously to 34.01 μ s (76.71%) and 167.79 μ s (23.29%) as the content of Pt(II) F_{20} TPPL increased to 2.0% in the H/G systems. These results indicated a higher energy transfer efficiency from the host to the guest with increasing Pt(II) F_{20} TPPL doping ratio.

The mechanoluminescence properties of pure *N*-hexyl Cz and the H/G NIR materials with different doping ratios of Pt(II) F_{20} TPPL into *N*-alkyl carbazole were measured by mechanical force at room temperature and the corresponding spectra are shown in Fig. 3. The mechanoluminescence band of pure *N*-hexyl Cz was detected at about 400–450 nm. The H/G systems with different doping ratios of Pt(II) F_{20} TPPL excited by mechanical force at room temperature also exhibited intense NIR

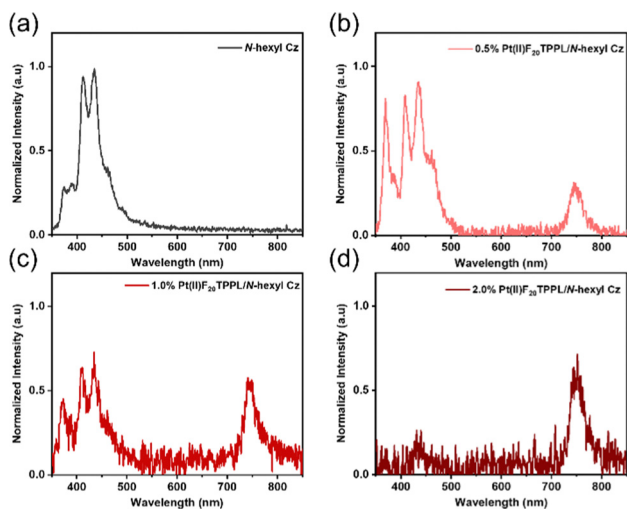


Fig. 3 (a) ML spectra of *N*-hexyl Cz, (b) 0.5% Pt(II) F_{20} TPPL/*N*-hexyl Cz, (c) 1.0% Pt(II) F_{20} TPPL/*N*-hexyl Cz and (d) 2.0% Pt(II) F_{20} TPPL/*N*-hexyl Cz.

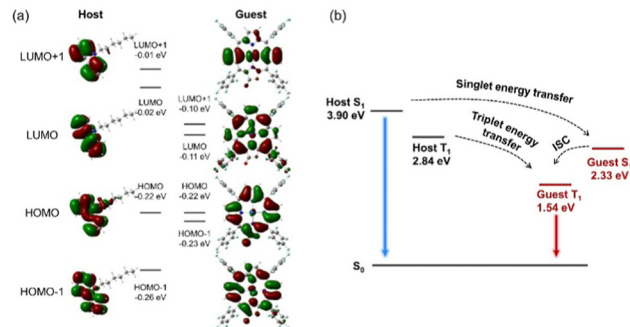


Fig. 4 (a) MO and (b) energy transfer diagrams.

luminescence. These profiles are identical to those of their photoluminescence (PL) spectra, which means the energy transfer process of ML is similar to that of PL. Intriguingly, when 2.0% (w/w) of Pt(II) F_{20} TPPL was doped into *N*-alkyl carbazole, the emission band at about 400–450 nm disappeared and a pure NIR ML band at 746 nm was realized. This result indicates that the energy transfer from the host to the guest is the dominant process in this H/G system and suggests that mechanical force is a superior stimulus type compared to light.

Theoretical calculations were performed at the PBE0/6-31g* level for a better understanding of the energy transfer process in this organic H/G system. The diagrams of frontier molecular orbitals (MO, HOMO and HOMO–1, LUMO and LUMO+1) and the host/guest energy transfer process are shown in Fig. 4. DFT results showed a good agreement between the calculated results and the experimental data. In phosphorescence spectra, the emission band at 736 nm indicates the transition energy is 1.67 eV, which is very close to the calculated energy of the guest's T_1 of 1.54 eV. Compared to the other calculated values illustrated in Fig. 4 (host S_1 , 3.90 eV; host T_1 , 2.84 eV; guest S_1 , 2.33 eV), it is demonstrated that the mechanophosphorescence originates from the exciton in the guest's triplet state transition to the guest's ground state. Besides, since the calculated energy of the exciton in the host's S_1 and the host's T_1 is 3.90 and 2.84 eV respectively, both higher than that in the guest's T_1 , the phosphorescence may originate from the host's S_1 or the host's T_1 . Based on our experimental results, there is no blue light but pure NIR luminescence, and this phosphorescence is most likely induced by the direct transition of the exciton in the host's T_1 to the guest's T_1 , followed by the emission from the guest's T_1 to the guest's S_0 .

NIR luminescence materials have extensive application prospects in biological imaging because of their unique properties of high penetration, high sensitivity, and safety to the detected objects. Compared with the mechanoluminescence of visible light, the NIR emission is invisible to the naked eye and can only be detected using a near-infrared camera, which is called "invisible mechanoluminescence". Accordingly, we examined this property by scratching the 2.0% Pt(II) F_{20} TPPL/*N*-hexyl Cz powder with a spatula in the dark, and obvious mechanoluminescence was observed using a near infrared camera (Fig. 5a), but no emission was detected when using an ordinary camera (similar to human eyes). This demonstrates that the 2.0%

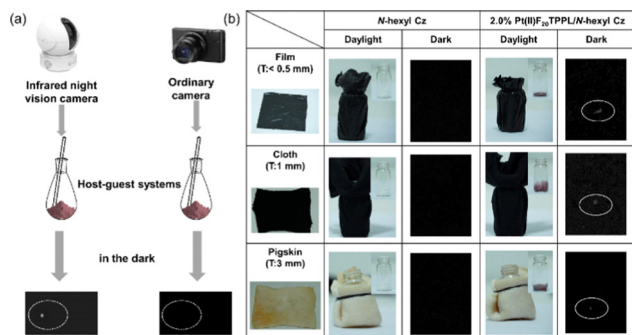


Fig. 5 (a) Image presenting the ML of 2.0% Pt(II)F₂₀TPPL/*N*-hexyl Cz with (left) a near infrared night camera and (right) an ordinary camera; (b) NIR ML images of 2.0% Pt(II)F₂₀TPPL/*N*-hexyl Cz in daylight and in the dark (the sample covered with black cloth (100% cotton, 0.03 mm), black film (polyethylene, 1 mm) and biological tissue (fresh pigskin, 3 mm)).

Pt(II)F₂₀TPPL/*N*-hexyl Cz doped materials could enable invisible mechanophosphorescence in the dark. Besides, NIR mechanoluminescence could penetrate biological tissue and thus enable visualization of biological internal stress, which enables the application of NIR ML materials in more practical fields, such as biomechanical monitoring. To demonstrate this, we tried to cover the surface of 2.0% Pt(II)F₂₀TPPL/*N*-hexyl Cz with black cloth, black film and biological tissue (fresh pigskin), respectively, scrape the material in the dark, and pass the near-infrared camera to detect NIR ML. NIR ML processes were all observed using a near-infrared camera in the H/G doped material 2.0% Pt(II)F₂₀TPPL/*N*-hexyl Cz after being covered by black cloth, black film and biological tissue (fresh pigskin) (Fig. 5b). Controlled experiments were also proceeded on the host material *N*-hexyl Cz, and no luminescence was detected. Therefore, the signal of NIR ML can penetrate biological tissue to realize the visualization of internal biological stress, which provides a potential material for mechanophosphorescence imaging in living organisms.

Conclusions

In summary, we have developed the first organic NIR mechanophosphorescence material based on the carbazole-Pt(II)F₂₀TPPL doped system. This H/G system has a rigid host skeleton and exhibits triplet exciton utilization in the emission process. Interestingly, changing the dopant ratio of Pt(II)F₂₀TPPL in the carbazole derivative could easily adjust the ratio of fluorescence–NIR phosphorescence. 2.0% (w/w) of Pt(II)F₂₀TPPL doped into *N*-alkyl carbazole could give the best phosphorescence purity and the longest phosphorescence lifetime. Theoretical calculations reveal the energy transfer process in which the phosphorescence in the doping system originated from the excitation of host matrices, followed by the energy transfer from the host to the guest, and realized by the luminescence of the guest. To our delight, this NIR mechanophosphorescence material can be applied as an invisible mechanoluminescence material since its emission could only be observed using an infrared detector, and also as a biophysical phosphorescence imaging material because of its high penetration. We believe that this work not only provides a feasible strategy

for fabricating the first organic NIR mechanophosphorescence material based on H/G systems with Pt(II)F₂₀TPPL, but also gives a theoretical understanding of the mechanism of organic NIR mechanophosphorescence. This may also provide us a new perspective on designing and developing more advanced organic NIR mechanophosphorescence materials with excellent properties in the future.

Author contributions

F. Hao and H. Wang conducted most of the experiments, analyzed the data and wrote the manuscript. D. Yu conducted the calculations. Z. Liu, T. Zhang and M. Shen helped in conducting the experiments. T. Yu designed the experiments and wrote the manuscript.

Conflicts of interest

There are no conflicts to declare.

Acknowledgements

The authors gratefully acknowledge the financial support from the NSF of China (62275217), the Chemistry and Chemical Engineering Basic Research and Innovation Cultivation Program of Qilu University of Technology (Shandong Academy of Sciences), the Fundamental Research Funds for the Central Universities, the Key Research and Development Program of Shaanxi Province (2020GXLH-Z-010), Chongqing Science and Technology Fund (cstc2020jcyjmsxmX0931), Guangdong Basic and Applied Basic Research Foundation (2021A1515010633), Ningbo Natural Science Foundation (202003N4060) and the National Aerospace Science Foundation of China (2020Z073053007).

Notes and references

- (a) B. P. Chandra and J. I. Zink, *Phys. Rev. B: Condens. Matter Mater. Phys.*, 1980, **21**, 816–826; (b) B. P. Chandra and J. I. Zink, *J. Chem. Phys.*, 1980, **73**, 5933–5941; (c) L. M. Sweeting, *Chem. Mater.*, 2001, **13**, 854–870.
- W. Li, Q. Huang, Z. Mao, J. Zhao, H. Wu, J. Chen, Z. Yang, Y. Li, Z. Yang, Y. Zhang, M. P. Aldred and Z. Chi, *Angew. Chem., Int. Ed.*, 2020, **59**, 3739–3745; W. Li, Q. Huang, Z. Mao, J. Zhao, H. Wu, J. Chen, Z. Yang, Y. Li, Z. Yang, Y. Zhang, M. P. Aldred and Z. Chi, *Angew. Chem.*, 2020, **132**, 3768–3774.
- (a) C. Wu, S. Zeng, Z. Wang, F. Wang, H. Zhou, J. Zhang, Z. Ci and L. Sun, *Adv. Funct. Mater.*, 2018, **28**, 1803168; (b) Z. Ma, J. Zhou, J. Zhang, S. Zeng, H. Zhou, A. T. Smith, W. Wang, L. Sun and Z. Wang, *Mater. Horiz.*, 2019, **6**, 2003–2008.
- (a) I. Sage, R. Badcock, L. Humberstone, N. Geddes, M. Kemp and G. Bourhill, *Smart Mater. Struct.*, 1999, **8**, 504–510; (b) I. Sage and G. Bourhill, *J. Mater. Chem.*, 2001, **11**, 231–245.

- 5 (a) S. Moon Jeong, S. Song, S.-K. Lee and B. Choi, *Appl. Phys. Lett.*, 2013, **102**, 051110; (b) S. M. Jeong, S. Song, K.-I. Joo, J. Kim, S.-H. Hwang, J. Jeong and H. Kim, *Energy Environ. Sci.*, 2014, **7**, 3338–3346.
- 6 (a) Y. Xie and Z. Li, *Chem*, 2018, **4**, 943–971; (b) Y. Zhuang and R.-J. Xie, *Adv. Mater.*, 2021, **33**, 2005925.
- 7 (a) Y. Xie and Z. Li, *Mater. Chem. Front.*, 2020, **4**, 317–331; (b) M. Liu, Q. Wu, H. Shi, Z. An and W. Huang, *Acta Chim. Sin.*, 2018, **76**, 246–258.
- 8 (a) C. R. Hurt, N. McAvoy, S. Bjorklund and N. Filipescu, *Nature*, 1966, **212**, 179–180; (b) S. Biju, N. Gopakumar, J. C. G. Bünzli, R. Scopelliti, H. K. Kim and M. L. P. Reddy, *Inorg. Chem.*, 2013, **52**, 8750–8758; (c) H.-Y. Wong, W.-S. Lo, W. T. K. Chan and G.-L. Law, *Inorg. Chem.*, 2017, **56**, 5135–5140.
- 9 (a) C.-H. Tseng, M. A. Fox, J.-L. Liao, C.-H. Ku, Z.-T. Sie, C.-H. Chang, J.-Y. Wang, Z.-N. Chen, G.-H. Lee and Y. Chi, *J. Mater. Chem. C*, 2017, **5**, 1420–1435; (b) A. Karimata, P. H. Patil, R. R. Fayzullin, E. Khaskin, S. Lapointe and J. R. Khusnutdinova, *Chem. Sci.*, 2020, **11**, 10814–10820.
- 10 (a) R. Nowak, A. Krajewska and M. Samoć, *Chem. Phys. Lett.*, 1983, **94**, 270–271; (b) S. Xu, T. Liu, Y. Mu, Y.-F. Wang, Z. Chi, C.-C. Lo, S. Liu, Y. Zhang, A. Lien and J. Xu, *Angew. Chem., Int. Ed.*, 2015, **54**, 874–878.
- 11 (a) J. Yang, X. Gao, Z. Xie, Y. Gong, M. Fang, Q. Peng, Z. Chi and Z. Li, *Angew. Chem., Int. Ed.*, 2017, **56**, 15299–15303; (b) K. K. Neena, P. Sudhakar, K. Dipak and P. Thilagar, *Chem. Commun.*, 2017, **53**, 3641–3644; (c) C. Arivazhagan, A. Maity, K. Bakthavachalam, A. Jana, S. K. Panigrahi, E. Suresh, A. Das and S. Ghosh, *Chem. – Eur. J.*, 2017, **23**, 7046–7051.
- 12 (a) H. Nakayama, J.-i Nishida, N. Takada, H. Sato and Y. Yamashita, *Chem. Mater.*, 2012, **24**, 671–676; (b) J.-i Nishida, H. Ohura, Y. Kita, H. Hasegawa, T. Kawase, N. Takada, H. Sato, Y. Sei and Y. Yamashita, *J. Org. Chem.*, 2016, **81**, 433–441.
- 13 (a) C. Wang, B. Xu, M. Li, Z. Chi, Y. Xie, Q. Li and Z. Li, *Mater. Horiz.*, 2016, **3**, 220–225; (b) Y. Xie, J. Tu, T. Zhang, J. Wang, Z. Xie, Z. Chi, Q. Peng and Z. Li, *Chem. Commun.*, 2017, **53**, 11330–11333.
- 14 (a) G. E. Hardy, J. I. Zink, W. C. Kaska and J. C. Baldwin, *J. Am. Chem. Soc.*, 1978, **100**, 8001–8002; (b) G. E. Hardy, W. C. Kaska, B. P. Chandra and J. I. Zink, *J. Am. Chem. Soc.*, 1981, **103**, 1074–1079.
- 15 (a) J. Yang, Z. Ren, Z. Xie, Y. Liu, C. Wang, Y. Xie, Q. Peng, B. Xu, W. Tian, F. Zhang, Z. Chi, Q. Li and Z. Li, *Angew. Chem., Int. Ed.*, 2017, **56**, 880–884; (b) Q. Sun, L. Tang, Z. Zhang, K. Zhang, Z. Xie, Z. Chi, H. Zhang and W. Yang, *Chem. Commun.*, 2018, **54**, 94–97.
- 16 (a) J. Guo, X.-L. Li, H. Nie, W. Luo, S. Gan, S. Hu, R. Hu, A. Qin, Z. Zhao, S.-J. Su and B. Z. Tang, *Adv. Funct. Mater.*, 2017, **27**, 1606458; (b) E. Ubba, Y. Tao, Z. Yang, J. Zhao, L. Wang and Z. Chi, *Chem. – Asian J.*, 2018, **13**, 3106–3121.
- 17 S. Hirata, Y. Sakai, K. Masui, H. Tanaka, S. Y. Lee, H. Nomura, N. Nakamura, M. Yasumatsu, H. Nakanotani, Q. Zhang, K. Shizu, H. Miyazaki and C. Adachi, *Nat. Mater.*, 2015, **14**, 330–336.
- 18 (a) P. Xiong, M. Peng and Z. Yang, *iScience*, 2021, **24**, 101944; (b) S. Liu, Y. Zheng, D. Peng, J. Zhao, Z. Song and Q. Liu, *Adv. Funct. Mater.*, 2023, **33**, 2209275.
- 19 (a) N. Tessler, V. Medvedev, M. Kazes, S. Kan and U. Banin, *Science*, 2002, **295**, 1506–1508; (b) K. S. Schanze, J. R. Reynolds, J. M. Boncella, B. S. Harrison, T. J. Foley, M. Bouguettaya and T.-S. Kang, *Synth. Met.*, 2003, **137**, 1013–1014; (c) E. L. Williams, J. Li and G. E. Jabbour, *Appl. Phys. Lett.*, 2006, **89**, 083506; (d) C. Yu, K. H.-Y. Chan, K. M.-C. Wong and V. W.-W. Yam, *Proc. Natl. Acad. Sci. U. S. A.*, 2006, **103**, 19652; (e) C. Y.-S. Chung, K. H.-Y. Chan and V. W.-W. Yam, *Chem. Commun.*, 2011, **47**, 2000–2002; (f) C. Y.-S. Chung and V. W.-W. Yam, *J. Am. Chem. Soc.*, 2011, **133**, 18775–18784; (g) Z. Guo, S. Park, J. Yoon and I. Shin, *Chem. Soc. Rev.*, 2014, **43**, 16–29; (h) H. Xiang, J. Cheng, X. Ma, X. Zhou and J. J. Chruma, *Chem. Soc. Rev.*, 2013, **42**, 6128–6185; (i) L. Yuan, W. Lin, K. Zheng, L. He and W. Huang, *Chem. Soc. Rev.*, 2013, **42**, 622–661.
- 20 (a) V. J. Pansare, S. Hejazi, W. J. Faenza and R. K. Prud'homme, *Chem. Mater.*, 2012, **24**, 812–827; (b) G. Qian and Z. Y. Wang, *Chem. – Asian J.*, 2010, **5**, 1006–1029.
- 21 Y. Avlasevich, C. Li and K. Müllen, *J. Mater. Chem.*, 2010, **20**, 3814–3826.
- 22 C. Jiao and J. Wu, *Synlett*, 2012, 171–184.
- 23 (a) C.-L. Ho, H. Li and W.-Y. Wong, *J. Organomet. Chem.*, 2014, **751**, 261–285; (b) K. Y. Zhang, S. Liu, Q. Zhao, F. Li and W. Huang, in *Luminescent and Photoactive Transition Metal Complexes as Biomolecular Probes and Cellular Reagents*, ed. K. K.-W. Lo, Springer Berlin Heidelberg, Berlin, Heidelberg, 2015, pp. 131–180, DOI: [10.1007/430_2014_166](https://doi.org/10.1007/430_2014_166).
- 24 (a) *The Porphyrin Handbook*, ed. K. M. Kadish, K. M. Smith and R. Guilard, Academic Press, San Diego, CA, 2000–2003; (b) N. V. S. D. K. Bhupathiraju, W. Rizvi, J. D. Batteas and C. M. Drain, *Org. Biomol. Chem.*, 2016, **14**, 389–408.
- 25 A. Barbieri, E. Bandini, F. Monti, V. K. Praveen and N. Armaroli, *Top. Curr. Chem.*, 2016, **374**, 47.
- 26 K. Koren, S. M. Borisov, R. Saf and I. Klimant, *Eur. J. Inorg. Chem.*, 2011, 1531–1534.
- 27 (a) S. M. Borisov, D. B. Papkovsky, G. V. Ponomarev, A. S. DeToma, R. Saf and I. Klimant, *J. Photochem. Photobiol., A*, 2009, **206**, 87–92; (b) O. S. Finikova, A. V. Cheprakov and S. A. Vinogradov, *J. Org. Chem.*, 2005, **70**, 9562–9572; (c) J. R. Sommer, A. H. Shelton, A. Parthasarathy, I. Ghiviriga, J. R. Reynolds and K. S. Schanze, *Chem. Mater.*, 2011, **23**, 5296–5304; (d) C. Borek, K. Hanson, P. I. Djurovich, M. E. Thompson, K. Aznavour, R. Bau, Y. Sun, S. R. Forrest, J. Brooks, L. Michalski and J. Brown, *Angew. Chem., Int. Ed.*, 2007, **46**, 1109–1112; (e) J. Currie Michael, K. Mapel Jonathan, D. Heidel Timothy, S. Goffri and A. Baldo Marc, *Science*, 2008, **321**, 226–228; (f) F. Niedermair, S. M. Borisov, G. Zenkl, O. T. Hofmann, H. Weber, R. Saf and I. Klimant, *Inorg. Chem.*, 2010, **49**, 9333–9342.
- 28 X.-S. Ke, H. Zhao, X. Zou, Y. Ning, X. Cheng, H. Su and J.-L. Zhang, *J. Am. Chem. Soc.*, 2015, **137**, 10745–10752.
- 29 (a) S. Saito and A. Osuka, *Angew. Chem., Int. Ed.*, 2011, **50**, 4342–4373; (b) Z. S. Yoon, J. H. Kwon, M.-C. Yoon,

- M. K. Koh, S. B. Noh, J. L. Sessler, J. T. Lee, D. Seidel, A. Aguilar, S. Shimizu, M. Suzuki, A. Osuka and D. Kim, *J. Am. Chem. Soc.*, 2006, **128**, 14128–14134.
- 30 (a) Y. Xie, P. Wei, X. Li, T. Hong, K. Zhang and H. Furuta, *J. Am. Chem. Soc.*, 2013, **135**, 19119–19122; (b) K. Fujino, Y. Hirata, Y. Kawabe, T. Morimoto, A. Srinivasan, M. Toganoh, Y. Miseki, A. Kudo and H. Furuta, *Angew. Chem., Int. Ed.*, 2011, **50**, 6855–6859.
- 31 (a) J. S. Lindsey, O. Mass and C.-Y. Chen, *New J. Chem.*, 2011, **35**, 511–516; (b) C.-Y. Chen, E. Sun, D. Fan, M. Taniguchi, B. E. McDowell, E. Yang, J. R. Diers, D. F. Bocian, D. Holten and J. S. Lindsey, *Inorg. Chem.*, 2012, **51**, 9443–9464.
- 32 (a) D. Bonifazi, M. Scholl, F. Song, L. Echegoyen, G. Accorsi, N. Armaroli and F. Diederich, *Angew. Chem., Int. Ed.*, 2003, **42**, 4966–4970; (b) H. S. Cho, D. H. Jeong, S. Cho, D. Kim, Y. Matsuzaki, K. Tanaka, A. Tsuda and A. Osuka, *J. Am. Chem. Soc.*, 2002, **124**, 14642–14654; (c) M. Pawlicki, M. Morisue, N. K. S. Davis, D. G. McLean, J. E. Haley, E. Beuerman, M. Drobizhev, A. Rebane, A. L. Thompson, S. I. Pascu, G. Accorsi, N. Armaroli and H. L. Anderson, *Chem. Sci.*, 2012, **3**, 1541–1547; (d) V. V. Diev, C. W. Schlenker, K. Hanson, Q. Zhong, J. D. Zimmerman, S. R. Forrest and M. E. Thompson, *J. Org. Chem.*, 2012, **77**, 143–159; (e) C. Jiao, K.-W. Huang, Z. Guan, Q.-H. Xu and J. Wu, *Org. Lett.*, 2010, **12**, 4046–4049.
- 33 (a) J. Iehl, M. Vartanian, M. Holler, J.-F. Nierengarten, B. Delavaux-Nicot, J.-M. Strub, A. Van Dorsselaer, Y. Wu, J. Mohanraj, K. Yoosaf and N. Armaroli, *J. Mater. Chem.*, 2011, **21**, 1562–1573; (b) N. Armaroli, G. Accorsi, F. Song, A. Palkar, L. Echegoyen, D. Bonifazi and F. Diederich, *Chem. Phys. Chem.*, 2005, **6**, 732–743; (c) T. V. Duncan, K. Susumu, L. E. Sinks and M. J. Therien, *J. Am. Chem. Soc.*, 2006, **128**, 9000–9001; (d) J. K. Sprafke, D. V. Kondratuk, M. Wykes, A. L. Thompson, M. Hoffmann, R. Drevinskis, W.-H. Chen, C. K. Yong, J. Kärnbratt, J. E. Bullock, M. Malfois, M. R. Wasielewski, B. Albinsson, L. M. Herz, D. Zigmantas, D. Beljonne and H. L. Anderson, *J. Am. Chem. Soc.*, 2011, **133**, 17262–17273.
- 34 (a) N. Kobayashi, H. Ogata, N. Nonaka and E. A. Luk'yanets, *Chem. – Eur. J.*, 2003, **9**, 5123–5134; (b) Ł. Łapok, M. Obłozza, A. Gorski, V. Knyukshto, T. Raichyonok, J. Waluk and M. Nowakowska, *Chem. Phys. Chem.*, 2016, **17**, 1123–1135.
- 35 (a) R. Kabe and C. Adachi, *Nature*, 2017, **550**, 384–387; (b) W. Li, Q. Huang, Z. Yang, X. Zhang, D. Ma, J. Zhao, C. Xu, Z. Mao, Y. Zhang and Z. Chi, *Angew. Chem., Int. Ed.*, 2020, **59**, 22645–22651.
- 36 C.-M. Che, Y.-J. Hou, M. C. W. Chan, J. Guo, Y. Liu and Y. Wang, *J. Mater. Chem.*, 2003, **13**, 1362–1366.
- 37 (a) Q. Li and Z. Li, *Acc. Chem. Res.*, 2020, **53**, 962–973; (b) J. Yang, M. Fang and Z. Li, *Acc. Mater. Res.*, 2021, **2**, 644–654; (c) L. Tu, Y. Xie and Z. Li, *J. Phys. Chem. Lett.*, 2022, **13**, 5605–5617; (d) A. Huang, Q. Li and Z. Li, *Chin. J. Chem.*, 2022, **40**, 2356–2370; (e) J. Gu, Z. Li and Q. Li, *Coord. Chem. Rev.*, 2023, **475**, 214872.
- 38 W. Li, Q. Huang, Z. Mao, Q. Li, L. Jiang, Z. Xie, R. Xu, Z. Yang, J. Zhao, T. Yu, Y. Zhang, M. P. Aldred and Z. Chi, *Angew. Chem., Int. Ed.*, 2018, **57**, 1272.
- 39 J. Yang, X. Wu, J. Shi, B. Tong, Y. Lei, Z. Cai and Y. Dong, *Adv. Funct. Mater.*, 2021, **31**, 2108072.